

Encounter times of chromatin loci influenced by polymer decondensation

A. Amitai¹ and D. Holcman²

¹*Department of Chemical Engineering and Institute for Medical Engineering & Science, Massachusetts Institute of Technology, Cambridge 02139, Massachusetts, USA*

²*Group of Applied Mathematics and Computational Biology, Ecole Normale Supérieure, 75005 Paris, France*



(Received 3 June 2017; revised manuscript received 11 February 2018; published 27 March 2018)

The time for a DNA sequence to find its homologous counterpart depends on a long random search inside the cell nucleus. Using polymer models, we compute here the mean first encounter time (MFET) between two sites located on two different polymer chains and confined locally by potential wells. We find that reducing tethering forces acting on the polymers results in local decondensation, and numerical simulations of the polymer model show that these changes are associated with a reduction of the MFET by several orders of magnitude. We derive here new asymptotic formula for the MFET, confirmed by Brownian simulations. We conclude from the present modeling approach that the fast search for homology is mediated by a local chromatin decondensation due to the release of multiple chromatin tethering forces. The present scenario could explain how the homologous recombination pathway for double-stranded DNA repair is controlled by its random search step.

DOI: [10.1103/PhysRevE.97.032417](https://doi.org/10.1103/PhysRevE.97.032417)

Repairing DNA double-strand breaks (DSBs) is a key step for cell survival. However, the underlying physical mechanism remains difficult to describe, mostly because it involves multiple molecular steps involving small (nanometer) and large (micrometer) scales. During the homologous recombination (HR) pathway, broken strands perform inside a large portion of the cell nucleus a random search for a homologous DNA template. Once this template is found, it will be used to copy the missing base pairs before repair [1]. As revealed by single-particle trajectories of chromatin [2,3], following a DSB, the broken locus dynamics is modified so that it can scan a larger area of the nucleus. This modification was attributed in part to chromatin decondensation and the release of tethering forces acting locally on the chromatin [4]. These changes could have consequences on the search for a homologous template. We present here polymer modeling and analytical tools to further characterize this search step.

We recall that search processes involving two loci located on the same polymers have been investigated in the context of polymer looping [5–8]. However, much less is known about the mean time for two monomers belonging to two different polymers. The multiple relaxation times associated with the polymer dynamics [9] shows that computing the looping time cannot be obtained by the classical activation escape from a potential well (representing the end-to-end distance energy) [10]. For a long polymer, the mean encounter time is influenced by the slowest internal relaxation times of the polymer [9]. However, it is not clear how these times contribute to the mean encounter time for two monomers located on two different polymers. In addition, in a confined environment, the probability distribution function of monomers varies along the polymer chain [11,12], which again can influence the search time.

To account for chromatin reorganization following DSB [4], we study here the random search of two monomers that belongs to two different monomers using the Rouse model [13] and the β -polymer [12]. Other polymer models of chromatin could be used for stochastic simulations, but deriving asymptotic laws

remains difficult for them [4,14–16] because they account for many physical forces. However, the two polymer models we will use here capture enough of the chromatin dynamics to be relevant. We focus on the local search time for homologous sequences located on two different polymers and restricted by external interactions, that we model as local potential wells. In that case, we derive asymptotic formulas for the encounter time of monomers located on two different polymers. To explore the range of validity of our analytical formulas, we compared them with stochastic simulations. These formulas show how the search time depends on the main physical parameters. Although this search step is far from covering the entire HR mechanism, it sheds some new lights on HR and shows how polymer condensation and physical constrains modulate the search time.

I. RESULTS

A. Search for Rouse polymer confined in a potential well

We recall that a Rouse polymer is a collection of monomers with positions $[\mathbf{R}_1, \mathbf{R}_2, \dots, \mathbf{R}_N]^T$, connected sequentially by harmonic springs [13]. We consider here two chains with same length N , where monomers are positioned at $\mathbf{R}_{i,n}$ ($n = 1, 2, \dots, N, i = a, b$), driven by Brownian motions and coupled to spring forces originating from the nearest neighbors. There are no direct forces between the two chains. The potential energy of the chains is the sum

$$\phi_{2\text{ch}} = \phi_{\text{Rouse}}^a(\mathbf{R}_{a,1}, \dots, \mathbf{R}_{a,N}) + \phi_{\text{Rouse}}^b(\mathbf{R}_{b,1}, \dots, \mathbf{R}_{b,N}), \quad (1)$$

where

$$\begin{aligned} \phi_{\text{Rouse}}^a(\mathbf{R}_{a,1}, \dots, \mathbf{R}_{a,N}) &= \frac{\kappa}{2} \sum_{n=1}^N (\mathbf{R}_{a,n} - \mathbf{R}_{a,n-1})^2, \\ \phi_{\text{Rouse}}^b(\mathbf{R}_{b,1}, \dots, \mathbf{R}_{b,N}) &= \frac{\kappa}{2} \sum_{n=1}^N (\mathbf{R}_{b,n} - \mathbf{R}_{b,n-1})^2, \end{aligned} \quad (2)$$

and the spring constant $\kappa = 3k_B T/b^2$ is related to the standard deviation b of the distance between adjacent monomers [13], with k_B the Boltzmann coefficient and T the temperature. In units of $k_B T$, we have $\kappa = 3/b^2$ and $D = 1/\gamma$, where γ is the friction coefficient. In the Smoluchowski's limit of the Langevin equation [17], the dynamics of monomer $\mathbf{R}_{i,n}$ is

$$\frac{d\mathbf{R}_{i,n}}{dt} = -D\nabla_{\mathbf{R}_{i,n}}\phi_{\text{Rouse}}^i + \sqrt{2D}\frac{d\mathbf{w}_{i,n}}{dt}, \quad (3)$$

where $i = a, b$, ϕ_{Rouse}^i are given in Eq. (2), $n = 1, \dots, N$, and $\mathbf{w}_{i,n}$ are independent three-dimensional white noises with mean zero and variance 1. We focus here on two monomers located on two different Rouse polymers a and b .

B. The MFET in a harmonic potential

The first result concerns the search time $\langle\tau_\epsilon\rangle$ between two monomers n_a, n_b to first enter into a ball of radius $\epsilon < b$ defined as the mean of

$$\tau_\epsilon = \inf\{t > 0 \text{ such that } |\mathbf{R}_{a,n_a}(t) - \mathbf{R}_{b,n_b}(t)| \leq \epsilon\}. \quad (4)$$

The two chains are restricted by a harmonic potential $\frac{1}{2}\rho \sum_{n=1}^N (\mathbf{R}_{a,n}^2 + \mathbf{R}_{b,n}^2)$ and the energy of the system is

$$\begin{aligned} \phi(\mathbf{R}_{a,1}, \dots, \mathbf{R}_{a,N}, \mathbf{R}_{b,1}, \dots, \mathbf{R}_{b,N}) \\ = \phi_{2\text{ch}} + \frac{\rho}{2} \sum_{n=1}^N (\mathbf{R}_{a,n}^2 + \mathbf{R}_{b,n}^2) \\ = \frac{1}{2} \sum_{p=0}^{N-1} (\kappa_p + \rho)(\mathbf{u}_{a,p}^2 + \mathbf{u}_{b,p}^2), \end{aligned} \quad (5)$$

where $\phi_{2\text{ch}}$ is defined in Eq. (1), $\mathbf{u}_{a,p}$ and $\mathbf{u}_{b,p}$ are the eigenvectors of the Rouse polymers a and b (see Appendix below), and the eigenvalues are

$$\kappa_p = 4\kappa \sin^2(p\pi/2N). \quad (6)$$

We derived (see Appendix below) the asymptotic formula in three dimensions for the MFET of the two middle monomers located on polymers a and b ,

$$\langle\tau_\epsilon^{\text{mid,mid}}\rangle = \frac{\pi^2}{D\epsilon} \left[\frac{1}{\sqrt{\kappa\rho}} - \frac{\rho}{N(8\kappa^2 + 2\kappa\rho)} \right]^{3/2} + C(\epsilon, N), \quad (7)$$

while for the end ones

$$\langle\tau_\epsilon^{\text{end,end}}\rangle = \frac{\pi^2}{D\epsilon} \left[\frac{2}{\sqrt{\kappa\rho}} - \frac{1}{\kappa} \left(1 + \frac{1}{N} \right) \right]^{3/2} + C(\epsilon, N). \quad (8)$$

These expressions are valid when the size of the confining potential $\rho^{-1/2}$ is larger than the characteristic length of a bond b , leading to the condition $\kappa/\rho > \frac{1}{4}$. When the potential wells approximate the confinement effect of a ball of radius A , this condition can be transformed using the calibration condition $\rho = 12/(A^4/b^2 + A^2)$ [18] into $A/b > \sqrt{0.5(\sqrt{5} - 1)}$. Note that the constant $C(\epsilon, N)$ is a $\mathcal{O}(1)$ correction. For the encounter of any two monomers, there is no closed analytical solution [Appendix formula (A41)]. To further explore the range of validity of these formulas, we use Brownian simulations of two polymers confined in a harmonic well [Fig. 1(a)]. As predicted

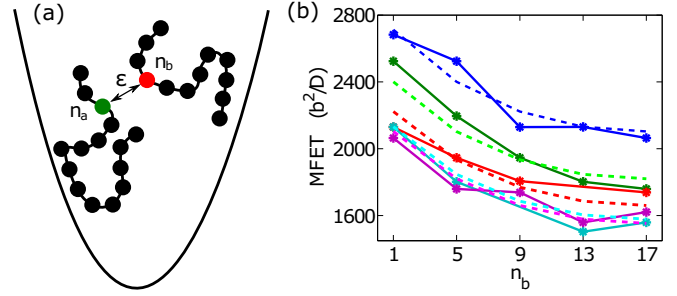


FIG. 1. MFET for two monomers in a harmonic potential. (a) Illustration of two Rouse polymers in a harmonic potential. In the model monomers n_a and n_b interact when they enter the ball of radius ϵ . (b) MFET for two monomers n_a and n_b belonging to two different polymers (length $N = 33$) in a harmonic well of strength $\rho = 0.01b^{-2}$, with $\epsilon = 0.01b$. The interacting monomer is n_b (x axis) and the different curves are computed for $n_a = 1$ (blue), $n_a = 5$ (green), $n_a = 9$ (red), $n_a = 13$ (cyan), $n_a = 17$ (magenta). The theoretical curves (dashed lines) agree with the simulation results and are computed from Eq. (42) with $\rho = 0.01b^{-2}$ and $C = 190b^2/D$.

by Eqs. (7) and (8), the MFET depends on the local position of the interacting monomers n_a and n_b that can be inside or at the end of the polymer chains.

We compared the numerical simulations with formula (A42) and fitted the constant term $C(\epsilon, N)$ to numerical simulation results [Fig. 1(b)]: for parameters $\epsilon = 0.01b$, $N = 33$, we found $C = 190b^2/D$. The analytical (dashed) and the numerical (points) results are compared in Fig. 1(b). The value of $C(\epsilon, N)$ contains higher order terms in the expansion of $\lambda_\epsilon^\epsilon$ [see Appendix, Eq. (A15)].

We conclude that the MFET is minimal for the two middle monomers. The middle monomers are localized in a confining region and their positions have a smaller standard deviation compared to the other monomers [11]. Finally, the MFET increases with the polymer length until it reaches an asymptotic value.

C. Following polymer decompaction, the local search time decays by two orders

We now explore the consequences of chromatin reorganization after DSB induction, where the dynamics of a chromatin locus in the proximity of the break is modified [19]. The changes are revealed by the subdiffusion behavior. Indeed, the mean-square displacement (MSD) behaves for short time increment $\Delta t \ll 1$ as $\langle |X(t + \delta t) - X(t)| \rangle \sim t^\alpha$ with $\alpha < 1$. Following break induction, the anomalous exponent α increases [4], reflecting also an increase in mobility and a local chromatin decondensation. These modifications can be accounted for by using the β model [12], which is a coarse-grained polymer model of chromatin that takes into account far away chromatin interactions. Long-range interactions could be mediated by protein-protein interactions, such as cohesin and condensin. We model the interaction using an energy between monomers given by

$$U_\beta(\mathbf{R}_1, \dots, \mathbf{R}_N, \beta) = \frac{1}{2} \sum_{l,m} A_{lm} \mathbf{R}_l \mathbf{R}_m, \quad (9)$$

with coefficients

$$A_{l,m} = \sum_{p=1}^{N-1} \tilde{\kappa}_p \alpha_p^l \alpha_p^m, \quad (10)$$

where α_p^m are the Rouse coefficients [see Appendix, Eq. (A8)], and

$$\tilde{\kappa}_p = 4\kappa \sin^\beta \left(\frac{p\pi}{2N} \right) \text{ for } p = 0, \dots, N-1. \quad (11)$$

The strength of interaction $A_{l,m}$ between monomers l and m decays with the distance $|l - m|$ along the chain. By definition, $1 < \beta \leq 2$ [12] and the Rouse polymer is recovered for $\beta = 2$, for which only nearest neighbors are connected. The model also relates the structure parameter β to the subdiffusive dynamics of a tagged monomer by the relation $\alpha = 1 - 1/\beta$. Thus, in a condensed polymer, the anomalous exponent of a monomer is lower than one belonging to a decondensed structure.

We reported recently that following break induction, the value of α increases from 0.3 to 0.48 [4]. Using the β -polymer model, we interpreted this change as a local decondensation of chromatin, confirmed in super-resolution microscopy [4,20]. For a polymer length of $N = 33$, the gyration radius (mean distance of the monomers to the center of mass) decreases from $\langle R_g \rangle = 2.34b$ for $\beta = 2$ to $\langle R_g \rangle = 1.4b$ for $\beta = 1.7$ and $\langle R_g \rangle = 1.21b$ for $\beta = 1.5$. We thus tested how the polymer decondensation influences the MFET for two middle monomers located on two different polymers with same length, when each is trapped by a potential well, separated by a distance r_0 [distance between the extremities where each polymer is anchored, Fig. 2(a)]. This scenario emulates a local homology

search. We first plotted the distribution of the middle monomers while decreasing the parameter β . We find that as β increases, the overlap of the two distributions decreases, as shown by the steady-state distributions of each monomer [Figs. 2(b) and 2(c)], obtained for various values of β .

Next, we estimated the MFET of the middle monomers of each chain for monomers $n_a = n_b = 17$. We find that increasing β from 1.3 to 2, leading to a decondensed polymer, decreases the MFET by two orders of magnitude [Fig. 2(d), thick black line]. This situation corresponds to a decondensation, where the polymer spring constant is fixed at $\approx 0.36k_B T/b^2$ between the middle monomer and its two neighbors. Finally, changing the anchoring distance r_0 affects the MFET by even larger orders of magnitude [Fig. 2(b)].

Interestingly, as the parameter β increases, the MFET does not always decrease. For a small anchoring distances $r_0 = 2b$, a condensed polymer is obtained by decreasing the value of β , thus leading to a reduced MFET [Fig. 2(d)]. We conclude that the encounter rate between two homologous sequences can be regulated by the average distance between monomers.

Possibly, after DSB induction, characterized by an increase in β [4], the spatial distribution of the broken loci is modified as described in Figs. 2(b) and 2(c), in a manner that depends on the tethering distance between polymers. This effect could be supported experimentally by considering the *S* phase and *G2*, where cohesin molecules maintain the sister chromatids together [21]. Due to their close proximity, sister chromatids could be used as templates for repair [22]. In general, the distribution of distances between two homologous loci is difficult to estimate. The median distance between cohesin binding sites is of the order of 16.5 kb for chromosome II of budding yeast [23]. A length $b = 30$ nm represents a monomer of size 3 kb [18], and 16.5 kb is a chain containing six monomers. The present result suggests that chromatin decondensation can significantly facilitate the encounter between monomers, and we predicted here a decay of the search by 2 orders of magnitude.

D. Removing the tethering forces applied on a polymer facilitates the local search

Chromatin strands are well localized [24] in the nucleus due to local interactions [25] imposed by the binding molecules such as Lamin A [26]. In this last section, we study the influence of local tethering forces on the search time. External forces acting on a tagged locus are characterized by a resulting tethering force with an effective spring constant k_c [Fig. 3(a)]. The consequence of this resulting force is to confine the locus motion [25].

We simulated the motion of several monomers, restricted by potential wells [Fig. 3(b)], where the energy for an interacting of monomer i is

$$U_i(\mathbf{R}_i) = \frac{1}{2}k(\mathbf{R}_i - \boldsymbol{\mu}_i)^2, \quad (12)$$

where μ_i is the center of the interacting well and k is the strength of the interaction. The total energy of an interacting Rouse polymer is

$$U_t = \phi_{2\text{ch}} + \sum_{i \text{ interacting}} U_i, \quad (13)$$

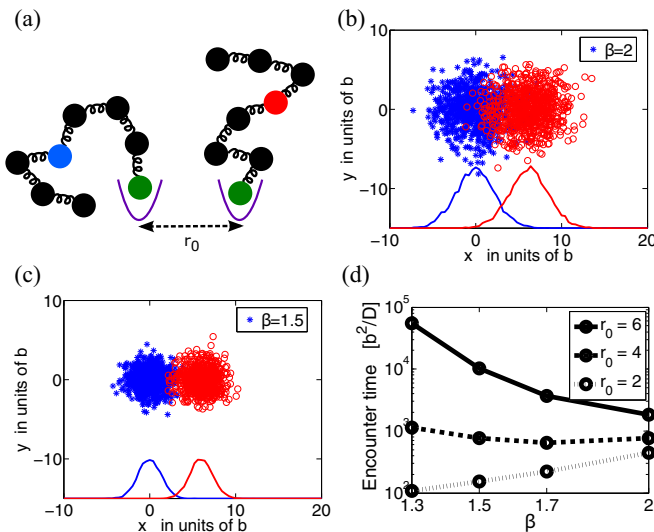


FIG. 2. Consequences of polymer condensation on search time. (a) Schematic representation of two polymers with anchored extremities separated by a distance r_0 . (b)–(c) Distribution of the middle monomers belonging to two different β polymers (red asterisk and blue circles) of length $N = 33$ in the XY plane. (b) $\beta = 2$ (Rouse) and (c) $\beta = 1.5$. (d) MFET for the two middle monomers plotted with respect to the parameter β and the distance r_0 . The radius is $\epsilon = 0.1b$ (y -axis units in b^2/D , where D is the diffusion coefficient).

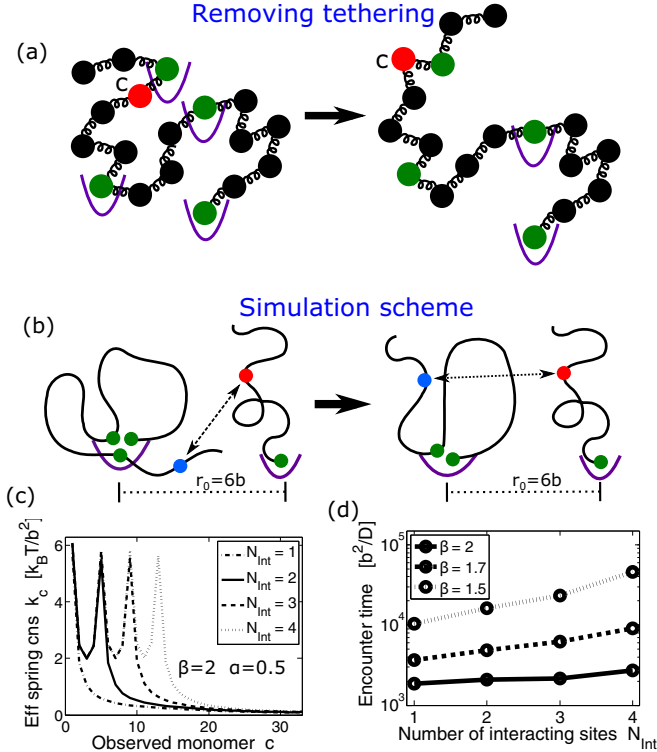


FIG. 3. Loss of local tethering interactions alters the MFET. (a) Two homologous polymers where a fraction of monomers (green) are interacting, modeled by fixed harmonic potential wells (purple). Following a DSB, these interactions are removed. (b) Scenario of two polymers (length $N = 33$), where the two middle monomers (blue and red) meet: only one extremity $n = 1$ belonging to one polymer is interacting with a potential well; for the other one, several monomers (green) are trapped ($n = 5, 9, 13$) at a well located at a fixed distance. The total number of interacting monomer is N_{Int} . (c) Estimation of the effective spring k_c for different monomers along the chain ($c = 1..33$) using formula (A43) for a Rouse polymer. One extremity interacts with a well (dashed-dotted line). We increase the number of interacting monomers N_{Int} , located at $n = 5$ (full line), $n = 9$ (dashed line), and $n = 13$ (dotted line). (d) MFET between the middle monomers for two β polymers and an increasing number of interacting sites.

where $\phi_{2\text{ch}}$ is defined in Eq. (1). We prerun the simulations to start with a polymer configuration that has reached a steady-state with respect to the energy U_t .

We study now how the additional interactions $\sum_i \text{interacting} U_i$ influence the dynamics of any monomers along the chain. Since in live-cell imaging one or two loci can be followed after being tagged, we follow the monomer of index c , and our goal is to recover the interactions of the polymer. We recall that the resulting force on a tracked locus [red bead in Fig. 3(a)] is computed [25] by the formula

$$\lim_{\Delta t \rightarrow 0} \mathbb{E} \left\{ \frac{\mathbf{R}_c(t + \Delta t) - \mathbf{R}_c(t)}{\Delta t} \middle| \mathbf{R}_c(t) = \mathbf{x} \right\} = -Dk_{cn}\mathbf{x}, \quad (14)$$

where $\mathbb{E}\{\cdot | \mathbf{R}_c = \mathbf{x}\}$ is the average over all polymer configurations under the condition that the tagged monomer is at position $\mathbf{R}_c = \mathbf{x}$. When only one monomer n is interacting with a potential [Eq. (12)], $k_{cn} = \frac{\kappa\kappa}{\kappa + (c-n)\kappa}$.

To investigate the consequences of removing punctual interactions, we simulated the search of two monomers belonging to two different polymers with the same length $N = 33$. The distance between the first monomers of each polymer is $r_0 = 6b$. In these simulations, we allow an increasing number of monomers of the polymers to interact at the origin [Fig. 3(b)], thus restricting the motion of the observed locus. We then estimated the parameter k_c from the simulated trajectories [Appendix, formula (A43)] [Fig. 3(c)] for different β polymers. When four monomers (at positions $n = 1, 5, 9, 13$) interact, we found [Fig. 3(c)] that $k_{c=15}^{N_{\text{Int}}=4} = 1.08k_B T/b^2$ for $\beta = 2$ and $k_{c=15}^{N_{\text{Int}}=4} = 1.73$ for $\beta = 1.5$. If only two monomers interact at positions $n = 1, 5$, the overall resulting interaction decays, characterized by $k_{c=15}^{N_{\text{Int}}=2} = 0.29k_B T/b^2$ (resp. $k_{c=15}^{N_{\text{Int}}=4} = 0.72k_B T/b^2$) for $\beta = 2$ (resp. $\beta = 1.5$).

To evaluate the influence of the number N_{Int} of interacting monomers on the MFET, we run Brownian simulations to compute the MFET between two middle monomers ($n_a = n_b = 17$) belonging to two different polymers of length $N = 33$. We find that the MFET increases with N_{Int} when the two polymer extremities are separated by a distance r_0 [Fig. 3(b)]. Interestingly, this increase depends on the polymer compaction, characterized by the parameter β : when $\beta = 1.5$, an increase of interacting monomers from $N_{\text{Int}} = 1$ to $N_{\text{Int}} = 4$ resulted in a 4.4-fold increase of the MFET [Fig. 3(d)]. We conclude that decreasing the tethering constant k_c , which represents the number of interactions of the DNA around the DSB (characterized by N_{Int}), results in a drastic reduction of the encounter time between two searching homologous sites.

Following DSB induction, experimental data confirmed that k_c is significantly decreased [4]. Thus, changes in the anchoring forces modify the locus dynamics that reflects the chromatin organization [25] [Fig. 3(a)].

II. CONCLUSION

To conclude, we derived here MFET formulas (7) and (8) for the search time between two monomers belonging to two polymer confined in harmonic wells. The MFET depends on the position of the monomers, chromatin condensation (parameter β and the anomalous exponent α), and tethering forces that represent binding forces, mediated by molecules such as CTCF or cohesin or other protein-protein interactions. The combination of polymer decondensation and releasing tethering forces can modulate and accelerate drastically the search time in a local environment (modeled here by potential wells). Polymer decondensation (increase in β) leads to a reduced MFET. Loss of local connectivities between monomers may arise from histone acetylation and local nucleosome eviction, as reported for DSBs in yeast [27]. This is likely to change the chromatin condensation and could accelerate the local search for homology.

ACKNOWLEDGMENT

A.A. acknowledges financial support from Massachusetts General Hospital Internal Fund 214931.

APPENDIX

In this Appendix, we present the derivation of the mean first encounter time (MFET) between two monomers that belongs to two different Rouse chains with same length N [formulas (2) and (3)], constrained in the same potential well of strength ρ . The MFET between the two middle monomers is given by

$$\langle \tau_{\epsilon}^{\text{mid,mid}} \rangle \approx \frac{\pi^2}{D\varepsilon} \left[\frac{2}{\pi\sqrt{\kappa\rho}} \tan^{-1} \left\{ 2\sqrt{\frac{\kappa}{\rho}} \tan \left(\frac{\pi}{2} - \frac{\pi}{2N} \right) \right\} + \frac{2}{N(4\kappa + \rho)} \right]^{3/2}, \quad (\text{A1})$$

while for the end ones

$$\langle \tau_{\epsilon}^{\text{end,end}} \rangle = \frac{\pi^2}{D\varepsilon} \left[\frac{4}{\pi\sqrt{\kappa\rho}} \tan^{-1} \left\{ 2\sqrt{\frac{\kappa}{\rho}} \tan \left(\frac{\pi}{2} - \frac{\pi}{2N} \right) \right\} - \frac{1}{\kappa} \right]^{3/2}. \quad (\text{A2})$$

In general, the MFET depends on the position of the searching monomers along the chain. The minimal MFET is achieved for the middle monomers of the chains when $\rho \ll 1$ (large domain).

Derivations of formulas (2) and (3)

To study the search process between two monomers n_a, n_b (located at a physical positions $\mathbf{R}_{n_a}, \mathbf{R}_{n_b}$) that belong to different polymers (a and b), we shall estimate the MFET $\langle \tau_{\epsilon} \rangle$ for these monomers to come into a distance $\varepsilon < b$, defined by the constraint

$$|\mathbf{R}_{n_a} - \mathbf{R}_{n_b}| \leq \varepsilon, \quad (\text{A3})$$

while the polymers evolve inside a confined ball, which is replaced here by a confined potential [18]. Indeed, the asymptotic computation for the time $\langle \tau_{\epsilon} \rangle$ is based on replacing the boundary on the polymer dynamics by a field of force (Fig. 1 of main text). Using this approximation, the polymer dynamics is modeled as a collection of monomers positioned at $\mathbf{R}_{i,n}$ ($n = 1, 2, \dots, N, i = a, b$), driven by Brownian motions and coupled to a spring forces of nearest neighbors. In Smoluchowski's limit of the Langevin equation [17], the dynamics of monomer $\mathbf{R}_{i,n}$ is

$$\frac{d\mathbf{R}_{i,n}}{dt} = -D\nabla_{\mathbf{R}_{i,n}}\phi(\mathbf{R}_{a,1}, \dots, \mathbf{R}_{a,N}) + \sqrt{2D}\frac{d\mathbf{w}_{i,n}}{dt} \quad (\text{A4})$$

for $n = 1, \dots, N$ and $i = a, b$, and $\mathbf{w}_{i,n}$ are independent three-dimensional white noises with mean zero and variance 1.

The final potential well is the sum of the Rouse and confined potentials for the two chains:

$$\begin{aligned} \phi(\mathbf{R}_{a,1}, \dots, \mathbf{R}_{a,N}) &= \phi_{\text{Rouse}}(\mathbf{R}_{a,1}, \dots, \mathbf{R}_{a,N}, \mathbf{R}_{b,1}, \dots, \mathbf{R}_{b,N}) \\ &+ \frac{\rho}{2} \sum_{n=1}^N (\mathbf{R}_{a,n}^2 + \mathbf{R}_{b,n}^2) \\ &= \frac{1}{2} \sum_{p=0}^{N-1} (\kappa_p + \rho)(\mathbf{u}_{a,p}^2 + \mathbf{u}_{b,p}^2), \end{aligned} \quad (\text{A5})$$

where

$$\begin{aligned} \phi_{\text{Rouse}}(\mathbf{R}_{a,1}, \dots, \mathbf{R}_{a,N}, \mathbf{R}_{b,1}, \dots, \mathbf{R}_{b,N}) \\ &= \phi_{\text{Rouse}}^a(\mathbf{R}_{a,1}, \dots, \mathbf{R}_{a,N}) + \phi_{\text{Rouse}}^b(\mathbf{R}_{b,1}, \dots, \mathbf{R}_{b,N}) \\ &= \frac{\kappa}{2} \sum_{n=1}^N (\mathbf{R}_{a,n} - \mathbf{R}_{a,n-1})^2 + \frac{\kappa}{2} \sum_{n=1}^N (\mathbf{R}_{b,n} - \mathbf{R}_{b,n-1})^2. \end{aligned} \quad (\text{A6})$$

The strength of the confined potential ρ can be adjusted so that the second moment properties match the ones obtained in a confinement ball (see [18]). The spring constant $\kappa = 3k_B T/b^2$ is related to the standard deviation b of the distance between adjacent monomers [13], k_B is the Boltzmann coefficient, and T the temperature. We recall that $\kappa_p = 4\kappa \sin^2(\frac{p\pi}{2N})$, and \mathbf{u}_p are the coordinates that diagonalize the quadratic potential well ϕ_{Rouse}^i [8],

$$\mathbf{u}_{i,p} = \sum_{n=1}^N \mathbf{R}_{i,n} \alpha_p^n, \quad (\text{A7})$$

where

$$\alpha_p^n = \begin{cases} \sqrt{\frac{1}{N}}, & p = 0, \\ \sqrt{\frac{2}{N}} \cos[(n-1/2)\frac{p\pi}{N}] & \text{otherwise.} \end{cases} \quad (\text{A8})$$

Asymptotic formula of the encounter time for two polymers in the same harmonic well

To compute the encounter time between two monomers, we extend the method we developed for a free polymer [8]. To derive the asymptotic formula for the MFET, we start with the stochastic dynamics of polymers in a confined domain:

$$\frac{d\mathbf{u}_{i,p}}{dt} = -D_p(\kappa_p + \rho)\mathbf{u}_{i,p} + \sqrt{2D_p}\frac{d\mathbf{w}_{i,p}}{dt}, \quad (\text{A9})$$

$$D_p = \begin{cases} D/N, & p = 0, \\ D & \text{otherwise} \end{cases} \quad (\text{A10})$$

for $p = 0, \dots, N-1$ and $i = a, b$, and $\mathbf{w}_{i,p}$ are independent three-dimensional white noises with mean zero and variance 1. The Fokker-Planck operator associated with the stochastic equation (A9) is

$$\begin{aligned} \mathcal{L}p &= \frac{D}{N} \sum_{i=a,b} \Delta_{\mathbf{u}_{i,0}} p(\mathbf{u}) + \nabla_{\mathbf{u}_{i,0}}(p(\mathbf{u})\nabla_{\mathbf{u}_{i,0}}\phi) \\ &+ D \sum_{i=a,b} \sum_{k=1}^{N-1} \Delta_{\mathbf{u}_{i,k}} p(\mathbf{u}) + \nabla_{\mathbf{u}_{i,k}}(p(\mathbf{u})\nabla_{\mathbf{u}_{i,k}}\phi), \end{aligned} \quad (\text{A11})$$

where $\mathbf{u} = (\mathbf{u}_{a,0}, \dots, \mathbf{u}_{a,N-1}, \mathbf{u}_{b,0}, \dots, \mathbf{u}_{b,N-1}) \in \Omega = \mathbb{R}^{6N}$. The absorbing boundary condition is $p(\mathbf{u}) = 0$ for $\mathbf{u} \in \partial S_{\epsilon}$, where

$$S_{\epsilon} = \left\{ \mathbf{u} \in \Omega \text{ s.t. } \left| \sum_{p=0}^{N-1} (\mathbf{u}_{a,p} \alpha_p^{n_a} - \mathbf{u}_{b,p} \alpha_p^{n_b}) \right| \leq \frac{\varepsilon}{2} \right\}. \quad (\text{A12})$$

The relation between the MFET $\langle \tau_{\epsilon} \rangle$ and the first eigenvalue λ_0^{ϵ} is [18,28]

$$\langle \tau_{\epsilon} \rangle \approx \frac{1}{D\lambda_0^{\epsilon}}. \quad (\text{A13})$$

To compute the first eigenvalue, we expand the perturbation formula [8,29]

$$\lambda_0^\epsilon = \lambda_0^0 + 4\pi\epsilon \int_S w_{\lambda_0^0}^2 dV_x + \mathcal{O}(\epsilon^2), \quad (\text{A14})$$

where $w_{\lambda_0^0} = |\mathbb{R}^{6N}|_\phi^{-1/2}$ is the eigenfunction associated with the zero eigenvalue $\lambda_0^0 = 0$, the volume element is $dV_x = e^{-\phi_h} dx_g$, and dx_g is the Euclidean measure over S [obtained by taking $\epsilon = 0$ in Eq. (A12)].

Following the derivation steps of [18], we obtain the following formula:

$$\lambda_0^\epsilon = \frac{4\pi\epsilon N^{3/2}}{2^{1/2}(2\pi)^3} \left[S(n_a, N, \rho) + S(n_b, N, \rho) - \frac{1}{\rho} \right]^{-3/2} + \mathcal{O}(\epsilon^2), \quad (\text{A15})$$

where

$$S(n, N, \rho) = \sum_{p=0}^{N-1} \frac{\cos\left[\left(n - \frac{1}{2}\right)\frac{p\pi}{N}\right]^2}{\kappa_p + \rho}. \quad (\text{A16})$$

The leading order term in (A15) was derived in [18], thus the novelty here concerns the approximation of the series $S(n, N, \rho)$, that we will describe below for $n = 1$ and $n = N/2$. First,

$$S(1, N, \rho) = \sum_{p=0}^{N-1} \frac{\cos\left(\frac{p\pi}{2N}\right)^2}{\kappa_p + \rho}. \quad (\text{A17})$$

To evaluate the series $S(1, N, \rho)$, we use the Euler-Maclaurin (EM) expansion formula:

$$\begin{aligned} F(f, a, b) &= \sum_{m=a}^b f(m, N, \rho) \approx \int_a^b f(m, N, \rho) dm \\ &+ \frac{f(a, N, \rho) + f(b, N, \rho)}{2} \\ &+ \frac{1}{12} [f'(b, N, \rho) - f'(a, N, \rho)], \end{aligned} \quad (\text{A18})$$

where

$$f(m, N) = \frac{\cos^2\left(\frac{p\pi}{2N}\right)}{1 + x \sin^2\left(\frac{p\pi}{2N}\right)}, \quad (\text{A19})$$

with $x = 4\kappa/\rho$. Thus $S(1, N, \rho) = \rho^{-1} \sum_{p=1}^{(N-1)} f(p, N)$. The integral term is computed as follows:

$$\begin{aligned} I &= \int_0^{N-1} \frac{\cos^2\left(\frac{y\pi}{2N}\right)}{1 + x \sin^2\left(\frac{y\pi}{2N}\right)} dy \\ &= \frac{2N}{\pi} \int_0^{(N-1)\pi/2N} \frac{\cos^2 t}{1 + x \sin^2 t} dt \\ &= \frac{2N}{\pi} \left[-\frac{t}{x} + \frac{\sqrt{1+x}}{x} \tan^{-1}\left(\sqrt{1+x} \tan t\right) \right]_0^{(N-1)\pi/2N} \\ &= \frac{1-N}{x} + \frac{2N\sqrt{1+x}}{x\pi} \left(gx, \frac{\pi}{2} - \frac{\pi}{2N} \right), \end{aligned} \quad (\text{A20})$$

where

$$(gx, t) = \tan^{-1}[\sqrt{1+x} \tan(t)]. \quad (\text{A21})$$

The derivative of function f is

$$\begin{aligned} f'(p, N) &= -\frac{(1+x)\pi \sin\left(\frac{p\pi}{N}\right)}{2N\left[1 + x \sin^2\left(\frac{p\pi}{2N}\right)\right]^2} \\ &= -\frac{2(1+x)\pi \sin\left(\frac{p\pi}{N}\right)}{\left[N2 + x + x \cos\left(\frac{p\pi}{N}\right)\right]^2} \end{aligned} \quad (\text{A22})$$

Substituting I from Eq. (A20) into the Maclaurin approximation (A18) with $a = 0$ and $b = N - 1$, we get

$$\begin{aligned} S(1, N, \rho) &\approx \frac{1-N}{x\rho} + \frac{2N\sqrt{1+x}}{x\rho\pi} \left(gx, \frac{\pi}{2} - \frac{\pi}{2N} \right) + \frac{1}{2\rho} \\ &+ \frac{1}{2\rho} \frac{\sin^2\left(\frac{\pi}{2N}\right)}{1 + x \cos^2\left(\frac{\pi}{2N}\right)} \\ &- \frac{(1+x)\pi \sin\left(\frac{\pi}{N}\right)}{6\rho\left[N2 + x - x \cos\left(\frac{\pi}{N}\right)\right]^2}, \end{aligned} \quad (\text{A23})$$

which can be approximated for $N \gg 1$:

$$S(1, N, \rho) \approx \frac{-N}{x\rho} + \frac{2N\sqrt{1+x}}{x\rho\pi} \left(gx, \frac{\pi}{2} - \frac{\pi}{2N} \right) + \frac{1}{2\rho}. \quad (\text{A24})$$

To estimate $S(N/2, N, \rho)$, we approximate

$$\begin{aligned} S(N/2, N, \rho) &= \sum_{p=0}^{N-1} \frac{\cos\left[(N-1)\frac{p\pi}{2N}\right]^2}{\kappa_p + \rho} \\ &= \sum_{p=0}^{N-1} \frac{\frac{1}{2}\{1 + \cos[(N-1)\frac{p\pi}{N}]\}}{\kappa_p + \rho} \\ &= \frac{1}{2} \sum_{p=0}^{N-1} \frac{1 + (-1)^p \cos\left(\frac{p\pi}{N}\right)}{\kappa_p + \rho} = s_1 + s_2, \end{aligned} \quad (\text{A25})$$

where

$$s_1(N, \rho) = \frac{1}{2} \sum_{p=0}^{N-1} \frac{1}{\kappa_p + \rho}, \quad (\text{A26})$$

and

$$s_2(N, \rho) = \frac{1}{2} \sum_{p=0}^{N-1} \frac{(-1)^p \cos\left(\frac{p\pi}{N}\right)}{\kappa_p + \rho}. \quad (\text{A27})$$

We now evaluate the first series s_1 using the EM formula: $s_1 = \rho^{-1} F(f_1, 0, N - 1)$, with

$$f_1(p, N, \rho) = \frac{1}{2} \frac{1}{x \sin\left(\frac{p\pi}{2N}\right)^2 + 1}. \quad (\text{A28})$$

The integral term is given by

$$\begin{aligned} I_1 &= \frac{1}{2} \int_{p=0}^{N-1} \frac{dp}{x \sin\left(\frac{p\pi}{2N}\right)^2 + 1} \\ &= \frac{N}{\pi} \int_0^{(N-1)\pi/2N} \frac{dt}{x \sin(t)^2 + 1} \\ &= \frac{N}{\pi\sqrt{1+x}} \left(gx, \frac{\pi}{2} - \frac{\pi}{2N} \right), \end{aligned} \quad (\text{A29})$$

while

$$f_1'(p, N, \rho) = -\frac{\pi x \sin\left(\frac{p\pi}{N}\right)}{4N\left[1 + x \sin\left(\frac{p\pi}{2N}\right)^2\right]}. \quad (\text{A30})$$

Thus

$$\begin{aligned} F(f_1, 0, N-1) &= I_1 + \frac{1}{2} \left[\frac{1}{2} + \frac{1}{2} \frac{1}{x \sin\left(\frac{(N-1)\pi}{2N}\right)^2 + 1} \right] \\ &\quad - \frac{\pi x \sin\left(\frac{(N-1)\pi}{N}\right)}{48N\left[1 + x \sin\left(\frac{(N-1)\pi}{2N}\right)^2\right]^2} \\ &= I_1 + \frac{1}{4} + \frac{1}{4} \frac{1}{x \cos\left(\frac{\pi}{2N}\right)^2 + 1} \\ &\quad - \frac{\pi x \sin\left(\frac{\pi}{N}\right)}{48N\left(1 + x \cos\left(\frac{\pi}{2N}\right)^2\right)^2}. \end{aligned} \quad (\text{A31})$$

We now evaluate the series s_2 using the EM formula: $s_2 = \rho^{-1} F(f_2, 0, N-1)$, with

$$f_2(p, N, \rho) = \frac{1}{2} \frac{(-1)^p \cos\left(\frac{p\pi}{N}\right)}{x \sin\left(\frac{p\pi}{2N}\right)^2 + 1}. \quad (\text{A32})$$

The integral term goes to zero because f_2 oscillates around zero with the index p . The boundary terms are

$$\begin{aligned} f_2(0, N, \rho) &= \frac{1}{2}, \\ f_2(N-1, N, \rho) &= -\frac{1}{2} \frac{\cos\left(\frac{\pi}{N}\right)}{x \cos\left(\frac{p\pi}{2N}\right)^2 + 1} \quad \text{for } N \text{ odd}, \\ f_2'(0, N, \rho) &= 0, \\ f_2'(N-1, N, \rho) &= \mathcal{O}(1/N^2). \end{aligned} \quad (\text{A33})$$

Thus

$$F(f_2, 0, N-1) = \frac{1}{4} + \frac{1}{4(x+1)} + \mathcal{O}\left(\frac{1}{N^2}\right). \quad (\text{A34})$$

Introducing (A31) and (A34) in (A25), and using that $N \gg 1$, we get

$$\begin{aligned} S(N/2, N, \rho) &= \frac{N}{\pi \rho \sqrt{1+x}} \left(g x, \frac{\pi}{2} - \frac{\pi}{2N} \right) \\ &\quad + \frac{1}{2\rho} + \frac{1}{2\rho} \frac{1}{x+1}. \end{aligned} \quad (\text{A35})$$

Substituting $x = 4\kappa/\rho$ into Eqs. (A24) and (A35), we find that

$$\begin{aligned} S(1, N, \rho) &\approx \frac{-N}{4\kappa} + \frac{N}{\pi \sqrt{\kappa\rho}} \tan^{-1} \left[2\sqrt{\frac{\kappa}{\rho}} \tan\left(\frac{\pi}{2} - \frac{\pi}{2N}\right) \right] \\ &\quad + \frac{1}{2\rho}, \end{aligned} \quad (\text{A36})$$

$$\begin{aligned} S(N/2, N, \rho) &\approx \frac{N}{2\pi \sqrt{\kappa\rho}} \tan^{-1} \left[2\sqrt{\frac{\kappa}{\rho}} \tan\left(\frac{\pi}{2} - \frac{\pi}{2N}\right) \right] \\ &\quad + \frac{1}{2\rho} + \frac{1}{8\kappa + 2\rho}. \end{aligned} \quad (\text{A37})$$

Using formula (A15) for the eigenvalue, related to the encounter of the two middle monomers ($n_a = N/2, n_b = N/2$), we get

$$\begin{aligned} \lambda_{0, \text{mid}, \text{mid}}^\epsilon &= \frac{4\pi \epsilon N^{3/2}}{2^{1/2}(2\pi)^3} \left[\frac{N}{\pi \sqrt{\kappa\rho}} \tan^{-1} \left\{ 2\sqrt{\frac{\kappa}{\rho}} \tan\left(\frac{\pi}{2} - \frac{\pi}{2N}\right) \right\} \right. \\ &\quad \left. + \frac{1}{4\kappa + \rho} \right]^{-3/2} + \mathcal{O}(\epsilon^2). \end{aligned} \quad (\text{A38})$$

The reciprocal of the first eigenvalue equation (A13) is the MFET:

$$\begin{aligned} \langle \tau_\epsilon^{\text{mid}, \text{mid}} \rangle &\approx \frac{\pi^2}{D\epsilon} \left[\frac{2}{\pi \sqrt{\kappa\rho}} \tan^{-1} \left\{ 2\sqrt{\frac{\kappa}{\rho}} \tan\left(\frac{\pi}{2} - \frac{\pi}{2N}\right) \right\} \right. \\ &\quad \left. + \frac{2}{N(4\kappa + \rho)} \right]^{3/2}. \end{aligned} \quad (\text{A39})$$

The eigenvalue for the encounter of the two end monomers ($n_a = 1, n_b = 1$) is

$$\begin{aligned} \lambda_{0, \text{end}, \text{end}}^\epsilon &= \frac{4\pi \epsilon N^{3/2}}{2^{1/2}(2\pi)^3} \left[\frac{2N}{\pi \sqrt{\kappa\rho}} \tan^{-1} \left\{ 2\sqrt{\frac{\kappa}{\rho}} \tan\left(\frac{\pi}{2} - \frac{\pi}{2N}\right) \right\} \right. \\ &\quad \left. - \frac{N}{2\kappa} \right]^{-3/2} + \mathcal{O}(\epsilon^2), \end{aligned} \quad (\text{A40})$$

and the MFET (A13) is

$$\begin{aligned} \langle \tau_\epsilon^{\text{end}, \text{end}} \rangle &\approx \frac{\pi^2}{D\epsilon} \left[\frac{4}{\pi \sqrt{\kappa\rho}} \tan^{-1} \left\{ 2\sqrt{\frac{\kappa}{\rho}} \tan\left(\frac{\pi}{2} - \frac{\pi}{2N}\right) \right\} \right. \\ &\quad \left. - \frac{1}{\kappa} \right]^{3/2}. \end{aligned} \quad (\text{A41})$$

In general, there are no close formulas for the MFET between any two monomers, but the reciprocal of the first eigenvalue [Eq. (A15)] can be used to obtain an estimation that could be compared to simulations:

$$\langle \tau_\epsilon^{n_a, n_b} \rangle = \frac{1}{\lambda_{0, n_a, n_b}^\epsilon}. \quad (\text{A42})$$

In summary, the MFET depends on the position of the searching monomers along the chain. The minimal MFET is achieved when the monomers are located at the middle of the chain when $\rho \ll 1$ (large domain). Finally, the MFET increases with the polymer length before reaching an asymptotic limit.

Empirical estimation of the tethering constant k_c

The effective spring constant k_c is estimated from trajectories of a tagged monomer at position $\mathbf{R}_c(t)$ using the empirical estimator

$$k_c = \frac{1}{D_c \Delta t 2T} \sum_{i=1}^d \sum_{k=1}^{T-1} \frac{R_c^i((k+1)\Delta t) - R_c^i(k\Delta t)}{R_c^i(k\Delta t) - \langle R_c^i \rangle}, \quad (\text{A43})$$

where d is the dimension, T is the number of points, Δt is the time step, and D the diffusion coefficient of the monomer.

- [1] A. Barzel and M. Kupiec, *Nat. Rev. Genet.* **9**, 27 (2008).
- [2] J. Miné-Hattab and R. Rothstein, *Nat. Cell Biol.* **14**, 510 (2012).
- [3] V. Dion, V. Kalck, C. Horigome, B. D. Towbin, and S. M. Gasser, *Nat. Cell Biol.* **14**, 502 (2012).
- [4] A. Amitai, A. Seeber, S. M. Gasser, and D. Holcman, *Cell Rep.* **18**, 1200 (2017).
- [5] G. Wilemski and M. Fixman, *J. Chem. Phys.* **58**, 4009 (1973).
- [6] G. Wilemski and M. Fixman, *J. Chem. Phys.* **60**, 866 (1974).
- [7] I. M. Sokolov, *Phys. Rev. Lett.* **90**, 080601 (2003).
- [8] A. Amitai, I. Kupka, and D. Holcman, *Phys. Rev. Lett.* **109**, 108302 (2012).
- [9] R. W. Pastor, R. Zwanzig, and A. Szabo, *J. Chem. Phys.* **105**, 3878 (1996).
- [10] K. Schulten, Z. Schulten, and A. Szabo, *J. Chem. Phys.* **74**, 4426 (1981).
- [11] A. Amitai, C. Amoruso, A. Ziskind, and D. Holcman, *J. Chem. Phys.* **137**, 244906 (2012).
- [12] A. Amitai and D. Holcman, *Phys. Rev. E* **88**, 052604 (2013).
- [13] M. Doi and S. F. Edwards, *The Theory of Polymer Dynamics* (Clarendon, Oxford, 1986).
- [14] D. W. Heermann, *Curr. Opin. Cell Biol.* **23**, 332 (2011).
- [15] D. W. Heermann, H. Jerabek, L. Liu, and Y. Li, *Methods* **58**, 307 (2012).
- [16] M. Fritsche, L. G. Reinholdt, M. Lessard, M. A. Handel, J. Bewersdorf, and D. W. Heermann, *PLoS One* **7**, e36282 (2012).
- [17] Z. Schuss, *Diffusion and Stochastic Processes. An Analytical Approach* (Springer-Verlag, New York, 2009).
- [18] A. Amitai and D. Holcman, *Phys. Rev. Lett.* **110**, 248105 (2013).
- [19] A. Seeber, V. Dion, and S. M. Gasser, *Genes Dev.* **27**, 1999 (2013).
- [20] M. H. Hauer, A. Seeber, V. Singh, R. Thierry, R. Sack, A. Amitai, M. Kryzhanovska, J. Eglinger, D. Holcman, T. Owen-Hughes, and S. M. Gasser, *Nat. Struct. Mol. Biol.* **24**, 99 (2017).
- [21] E. Revenkova and R. Jessberger, *Chromosoma* **115**, 235 (2006).
- [22] D. Zickler and N. Kleckner, *Cold Spring Harb. Perspect. Biol.* **7**, a016626 (2015).
- [23] C. K. Schmidt, N. Brookes, and F. Uhlmann, *Genome Biology* **10**, R52 (2009).
- [24] C. Zimmer and E. Fabre, *J. Cell Biol.* **192**, 723 (2011).
- [25] A. Amitai, M. Toulouze, K. Dubrana, and D. Holcman, *PLoS Comput. Biol.* **11**, e1004433 (2015).
- [26] I. Bronshtein, E. Kepten, I. Kanter, S. Berezin, M. Lindner, A. B. Redwood, S. Mai, S. Gonzalo, R. Foisner, Y. Shav-Tal, and Y. Seeber, *Nat. Commun.* **6**, 8044 (2015).
- [27] J. Renkawitz, C. A. Lademann, and S. Jentsch, *Nat. Rev. Mol. Cell Biol.* **15**, 369 (2014).
- [28] A. Amitai, I. Kupka, and D. Holcman, *J. Stat. Phys.* **153**, 1107 (2013).
- [29] I. Chavel and E. A. Feldman, *J. Duke Math.* **56**, 399 (1988).